International Soil and Water Conservation Research 8 (2020) 195–204

Contents lists available at ScienceDirect

International Soil and Water Conservation Research

journal homepage: www.elsevier.com/locate/iswcr

Original Research Article

The application of proximal visible and near-infrared spectroscopy to estimate soil organic matter on the Triffa Plain of Morocco

Ayoub Lazaar [a, *], Abdul Mounem Mouazen [b], Kamal EL Hammouti [a], Michael Fullen [c], Biswajeet Pradhan [d], Muhammad Sohail Memon [e], Karim Andich [f], Abdelilah Monir [g]

[a] Laboratory of Applied Geosciences, Department of Geology, Faculty of Science, Mohammed First University, Oujda, Morocco
[b] Department of Environment, Ghent University, Coupure Links 653, 9000 Gent, Belgium
[c] Faculty of Science and Engineering, University of Wolverhampton, Wolverhampton, WV1 1LY, United Kingdom
[d] Center for Advanced Modelling and Geospatial Information Systems (CAMGIS), Faculty of Engineering and Information Technology, University of Technology Sydney, Sydney, 2007, NSW, Australia
[e] Faculty of Agricultural Engineering, Sindh Agriculture University, Tandojam, 70060, Pakistan
[f] Laboratory of Applied Geomatics and Soil Science, National Institute of Agronomic Research (INRA), Oujda, Morocco
[g] Department of Mathematics, EDP and Scientific Computing Team, Moulay Ismail University, Méknes, Morocco

ARTICLE INFO

Article history:
Received 14 October 2019
Received in revised form
13 April 2020
Accepted 15 April 2020
Available online 21 April 2020

Keywords:
Soil organic matter
VIS-NIR spectroscopy
Reflectance spectra
SOM estimation
SOM analysis

ABSTRACT

Soil organic matter (SOM) is a fundamental soil constituent. The estimation of this parameter in the laboratory using the classical method is complex time-consuming and requires the use of chemical reagents. The objectives of this study were to assess the accuracy of two laboratory measurement setups of the VIS-NIR spectroscopy in estimating SOM content and determine the important spectral bands in the SOM estimation model. A total of 115 soil samples were collected from the non-root zone (0–20 cm) of soil in the study area of the Triffa Plain and then analysed for SOM in the laboratory by the Walkley –Black method. The reflectance spectra of soil samples were measured by two protocols, Contact Probe (CP) and Pistol Grip (PG)) of the ASD spectroradiometer (350–2500 nm) in the laboratory. Partial least squares regression (PLSR) was used to develop the prediction models. The results of coefficient of determination (R^2) and the root mean square error (RMSE) showed that the pistol grip offers reasonable accuracy with an $R^2 = 0.93$ and RMSE = 0.13 compared to the contact probe protocol with an $R^2 = 0.85$ and RMSE = 0.19. The near-Infrared range were more accurate than those in the visible range for predicting SOM using the both setups (CP and PG). The significant wavelengths contributing to the prediction of SOM for (PG) setup were at: 424, 597, 1432, 1484, 1830,1920, 2200, 2357 and 2430 nm, while were at 433, 587, 1380, 1431, 1929, 2200 and 2345 nm for (CP) setup.

1. Introduction

The soil is a vital and non-renewable natural resource with potentially rapid degradation rates and extremely slow formation and regeneration processes. It is a complex, heterogeneous and self-organized system, extremely variable in chemical and physical composition (Lavelle et al., 2007) both spatially and temporarily. The physicochemical properties of soils determine their potential and limitations for agricultural use (Leone et al., 2012; Tümsavaş, Tekin, Ulusoy, & Mouazen, 2018), but these vary inter- and intra-fields. Whatever the scale is, it is essential to predict and map variability accurately in order to manage farm input resources.

Soil organic matter (SOM) is an important parameter for soil functions and is an indicator of soil fertility. It takes a major role in forming and stabilizing soil aggregates for the long term sustainability (Memon et al., 2018; Six, Conant, Paul, & Paustian, 2002). Powlson, Brookes, Whitmore, Goulding, and Hopkins (2011) and Hong et al. (2018) mentioned that SOM is the decisive factor of soil fertility, and its content is directly related to the soil fertility properties, such as nutrient holding capacity, soil microbial quantity and activity, soil water-holding capacity, nutrient use efficiency and crop yield. St Luce et al. (2014) indicated that assessment and

* Corresponding author. Department of Geology, Mohammed First University, Oujda, Morocco.
E-mail address: lazaar.ayoub1@gmail.com (A. Lazaar).

https://doi.org/10.1016/j.iswcr.2020.04.005

monitoring of SOM are important for determining and developing management practices that will enhance and maintain the productivity of agricultural soils. Jakab, Rieder, Vancsik, and Szalai (2018) noted that natural SOM systems can be disturbed by physical and chemical effects, such as agricultural land use. In north-east Morocco, like other parts of the world, intensive agriculture a common practice to respond to the strong demand for food, leading to a non-rational use of fertilizers and the increase soil erosion, causing loss of SOM. That is why, it necessary to identify and understand the Spatio-temporal distribution of SOM in order to optimize the use of farm input (e.g., fertilizers, seed rate) on a specific site.

The use of traditional soil analytical techniques in laboratories in order to identify and determine SOM and other soil physicochemical properties is complicated, expensive and requires much of time and effort. Thus, alternative or complimentary techniques for soil characterization are needed for both *in situ* and laboratory conditions. Currently, visible-near-infrared and shortwave-infrared (VIS-NIR-SWIR) spectroscopy represents an alternative method for soil analysis and quantification, is a fast, non-destructive, environmentally friendly (does not use the chemical reagents), repeatable analytical technique and requires minimal sample preparation (Gholizadeh, Borůvka, Saberioon, & Vasat, 2013; Lazaar et al., 2019; Leone et al., 2012; Sun, Li, & Niu, 2018). It is widely used to measure key soil properties, such as soil organic carbon (SOC) (Gomez, Viscarra Rossel, & McBratney, 2008; Jiang, Chen, Guo, Fei, & Qi, 2016; Stevens et al., 2006, 2010; Xie, Yang, Drury, Yang, & Zhang, 2011), calcium carbonates ($CaCO_3$) (Ben-Dor & Banin, 1990; Cécile et al., 2008; Lagacherie, Baret, Feret, Madeira Netto, & Robbez-Masson, 2008), texture (Curcio, Ciraolo, D'Asaro, & Minacapilli, 2013; Lagacherie et al., 2008; Virgawati et al., 2018), and total or organic nitrogen (Gomez, Oltra-Carrió, Bacha, Lagacherie, & Briottet, 2015; He, Song, Pereira, & Gómez, 2005; Tümsavaş et al., 2018). Vašát et al. (2014) indicated that SOM is one of the main soil parameters that can be predicted with reflectance spectroscopy, as it affects notably the shape and nature of soil reflectance spectra (Gholizadeh et al., 2013; Gomez, Lagacherie, & Coulouma, 2008; Gomez, Viscarra Rossel, et al., 2008).

VIS-NIR-SWIR proximal sensing is based on the development of empirical models in which the concentration of soil constituent is predicted from complex spectral data (Coûteaux, Berg, & Rovira, 2003) including visible (VIS: 350–780 nm), near-infrared (NIR: 780–1100 nm) and short-wave infrared (SWIR: 1100–2500 nm) bands. Xie et al. (2011) discovered that the evolution of advances in chemometric methods goal the application of NIR spectroscopy technique in Soil Science. Different data mining techniques are used to extract useful and quantitative information from soil spectra, including machine-learning and regression techniques. Many reports demonstrated the superiority of the machine-learning techniques over regression techniques in soil analysis (Mouazen, Kuang, De Baerdemaeker, & Ramon, 2010; Nawar & Mouazen, 2017; Viscarra Rossel & Behrens, 2010), as they account for the non-linear spectral responses. However, many authors have shown that the partial least squares regression (PLSR) method as one of the best chemometric tools for predicting SOM (Bao, Wu, Ye, Yang, & Zhou, 2017; Chen, Pan, Chen, & Lu, 2011; Demattê, Ramirez-Lopez, Marques, & Rodella, 2017; He et al., 2005; Hong et al., 2018; Jakab et al., 2018). Apart from the modelling method applied, the quality of prediction is associated with three major factors: (i) soil sample preparation (e.g., processed or fresh soil samples), (ii) the instrument used for measurement (e.g., type of detector, spectral range, spectral resolution, light source used), and (iii) the applied laboratory protocols (Ben-Dor, Ong, & Lau, 2014; Gholizadeh, Carmon, Klement, Ben-Dor, & Borůvka, 2017; Rosero-vlasova, Péerez-Cabello, Lloveria, & Vlassova, 2016).

The aim of this work was to investigate the performance of VIS-NIR diffuse reflectance spectroscopy for the prediction of SOM in irrigated land of Triffa Plain of the north-east Morocco, using two protocols (Contact Probe (CP) and Pistol Grip (PG)) of measuring the reflectance spectra of the ASD FieldSpec III spectroradiometer. The study also aimed to determine the important spectral bands in the SOM prediction model of each protocol.

2. Material and methods

2.1. Study area and soil sampling

The irrigated perimeter of the Triffa Plain is located in the eastern Morocco (longitude 34°56′32.67″ N; latitude 2°24′05.95″ W) and cover an area of 560 km^2 with an altitude of 120–200 m above sea level (Fig. 1). The study area has a semi-arid climate with an average annual precipitation of 330 mm and mean temperature of 24 °C (Fekkoul, 2012). It represents the most fertile and productive agricultural region in the north-eastern Morocco. It is characterized by a diversity of soil types, represented mainly by the isohumic, rendzina, brown calcareous, fersialitic, less-developed, and hydromorphic soil (Lazaar, 2016). The isohumic soils correspond to thick soils with the black to brown colour, rich in Organic Matter (OM) with a lumpy structure and fertile agricultural lands. Rendzina soil types are also called calcimagnesian soils. They are developed from calcareous parent rocks, in which their OM is rapidly decomposed and the humidification process is blocked due to the excess of calcium that slows down alteration (Aubert, 1965). Calcareous brown soils are also developed from calcareous parent rocks with an upper organo-mineral horizon (A1). These soils are stony, deep and provide the best agricultural land in the Triffa Plain. Red soils, known as fersialitic soils, are fertile, but are very erodible by both wind and water. Hydromorphic soils and less-developed soils represent only a small position in the study area (Lazaar, 2016).

The sampling locations were chosen with a sampling scheme prepared with ArcGIS software in which the most sampling locations are representative of the major landforms and land cover types of the study area. Soil sampling was carried out during August 2018. This time period was selected to ensure a high proportion of bare soils within the study area after harvest and ploughing of most of cereals, sugar beets and potato fields. A total of 115 soil samples were collected from the topsoil zone (0–20 cm) of the different soil types situated in this plain (isohumic, rendzina, brown calcareous, fersialitic, less-developed, and hydromorphic soils) with at a density of one sample per 1.5 km^2 using a mechanical auger while the localization of soil samples was recorded by a Garmin GPS portable. The totality of soil sampling was carried in a vast plain landforms with soft topography dominated the study area and in two land-use types: in agricultural lands covered by several fields of cereals (35 soil samples), sugar beets (10 soil samples), potatoes (10 soil samples), citrus (15 soil samples), olives (10 soil samples) and watermelon (8 soil samples) and in the uncultivated bare-land (27 soil samples). Each soil sample was then split into two sub-samples: one was used for the laboratory spectral measurements, while the other was used for the laboratory physicochemical analysis of five soil properties: SOM, soil pH, Calcium carbonates ($CaCO_3$), available phosphorus (P_5O_2) and the electrical conductivity (EC). The SOM was determined using the Walkley–Black method (Walkley & Black, 1934) and the soil pH was measured potentiometrically in distilled water (Lazaar et al., 2019). The calcium carbonates were determined by the Bernard calcimeter method according to the AFNOR NF P 94-048 (2003) norm. For the available phosphorus of the soil was extracted with a combined solution of 0.1 M HCl and 0.03 M NH4F and the measurements were made using an ultraviolet (UV) spectrophotometer (Sacko, Sanogo,

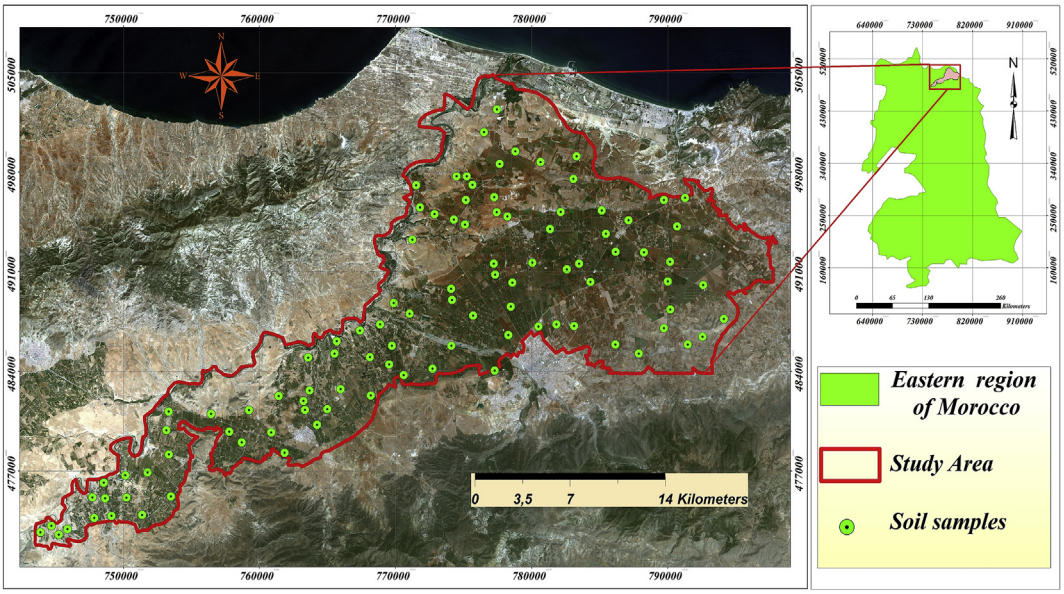

Fig. 1. The study area location in irrigated perimeter of the Triffa Plain (north-east of Morocco).

Konare, Ba, & Diakite, 2018). Electrical conductivity was measured by 1: 5 soil: H_2O extract method (Rayment & Higginson, 1992).

2.2. Spectral measurement and pre-processing

All collected soil samples were air-dried at 100 °C for 24 h and then sieved through at 2 mm sieve, and then stored in optical-glass Petri dishes with a diameter of 95 mm and a thickness of 15 mm. The reflectance spectra of the soil samples were measured in the laboratory in the visible (VIS: 350–780 nm), near-infrared (NIR: 780–1100 nm) and short-wave infrared (SWIR: 1100–2500 nm) ranges using an ASD FieldSpec III Pro spectroradiometer, with a spectral resolution of 2 nm for the region situated between 350 and 1050 nm and 10 nm for the range between 1050 and 2500 nm (Gholizadeh et al., 2017). Two laboratory setups were used for measuring soil spectra: (i) the contact probe (CP) and (ii) the pistol grip with illuminator lamp (PG) (Fig. 2).

For the first configuration (Fig. 2a), before each measurement, the surface of soil samples placed in the Petri dishes must be pressed with a spatula to ensure maximum diffuse reflectance and to obtain a low signal-to-noise ratio (Mouazen, Maleki, De Baerdemaeker, & Ramon, 2007; Xu, Shi, Wang, & Zhao, 2016). A high-intensity contact probe internal light source composed of a reflectorized halogen lamp aligned at 12° with a measurement spot size of 10 mm and attached with an optical probe cable of the spectroradiometer, were pasted directly on each soil surface. The scan of soil spectra was repeated 10 times at five random points of the soil sample, in order to minimize the risk of shadows and errors associated with stray light (Rosero-vlasova et al., 2016). The contact probe setup was calibrated with a white reference (spectralon) once every 10 measurements.

For the second setup, measurements of soil spectra were conducted with an optical probe integrated into a pistol grip with an illuminator Halogen lamp of 65 W as a relative source illumination. This halogen lamp was fixed vertically with a height of 17 cm to the Petri dish, while the pistol grip was attached to another tripod with an aiming angle of 45° relative to the vertical axis and a height of 7 cm (Fig. 2b). The Petri dishes of soil samples were deposited in a circle previously drawn in the manipulation table in order to minimize the error of measurement, and before each scan of soil spectra, the sensor was calibrated with the white reference, and recalibrate every 10 successive measurements (10 soil samples).

Fig. 2. Soil spectra measurement with two laboratory setups: (a) Contact probe (CP) setup, (b) pistol grip (PG) with illuminator lamp setup, and (c) geometry configuration of pistol grip (PG) with illuminator lamp setup.

In order to enhance the SOM model prediction, the spectroscopic data acquired in the two-setups of laboratory measurement needed several pre-treatments. The aim of this pre-processing was to remove the undesired variation in the data (Leone et al., 2012). Spectral regions 350–399 nm and 2451–2500 nm were removed because they are affected by the noise. The measured reflectance spectra (400–2450 nm) of soil samples were transformed into absorbance (log 1/R) to improve correlation to sample concentration (Bellon-Maurel, Fernandez-Ahumada, Palagos, Roger, & McBratney, 2010; Ji et al., 2016). Several pre-treatments were considered such as the standard normal variate and detrending for reducing scatter and particles size effects and to remove the linear or curvilinear of the spectrum (Barnes, Dhanoa, & Lister, 1989), the mean and maximum normalization, the multiplicative scatter, and the first and second derivate (Fystro, 2002; Mouazen, Saeys, Xing, De Baerdemaeker, & Ramon, 2005; Van Waes, Mestdagh, Lootens, & Carlier, 2005). Moreover, in order to create a robust model prediction of SOM, many pre-treatment methods were tested, such as the standard normal variate (SNV), detrend, a combination of SNV and detrend, multiplicative scatter and maximum normalization. Finally, the transformation of reflectance into absorbance (log1/R) and the applied of first derivative transformation with the Savitsky-Golay smoothing algorithms (Savitzky & Golay, 1964) with a window size of 10 and polynomial of order 2 was chosen as the optimum data pre-treatment method. All pre-treatments and procedures were conducted using Unscrambler 10.4 software.

2.3. Partial least squares regression (PLSR) analysis and IDW GIS-Kriging

2.3.1. Partial least squares regression method

PLSR is the widely most used method for spectral calibration and prediction (Ji et al., 2016) because it gives more stronger correlated results compared to the different multivariate methods (Bogrekci & Lee, 2004; Chang, Laird, Mausbach, & Hurburgh, 2001; Tümsavaş et al., 2018). In this study, the PLSR technique coupled with cross-validation was used to create and establish a model prediction between the soil spectra of soil samples and the reference value of SOM. Two model calibrations were developed, one for the contact probe configuration and the second for the pistol grip configuration. The selection criteria for evaluating the performance of model prediction is based on coefficient of determination (R^2) value, and the root means square error of prediction (RMSEP) (Aïchi et al., 2009; Mouazen et al., 2007; Viscarra Rossel, Walvoort, McBratney, Janik, & Skjemstad, 2006).

Before running the analysis of SOM prediction using the PLSR method for the two measurement protocols, the data set was divided into a calibration set (75 % or 85 soil samples) will allow us to create the model and a validation set (25% or 30 soil samples) which measures the error of the final model on data it has never seen before. For this validation set cannot be considered to be completely independent from the calibration set due to the spatial autocorrelation in spectral data or SOM content arising between samples situated in close proximity or belonging to the same field.

2.3.2. Spatial variability mapping of SOM with IDW interpolation method

IDW is one of the most applied and deterministic interpolation techniques used in soil science for mapping the spatial variability of soil proprieties (Xu, Li, Li, Lu, & Wang, 2013). The mapping of SOM variability in the study area was created using ArcGIS software, using the inverse distance weighting (IDW) interpolation method, in order to evaluate the influence of the laboratory procedures on the statistical model predicted for the (CP) and (PG) setups.

2.4. Statistical analysis

The data of soil chemical analysis were identified by several statistical parameters such as mean, maximum, minimum, standard deviation, variance, median range, skewness and kurtosis. Mean, maximum, minimum and median were used to describe the central tendency and distribution of soil parameter values. The standard deviation, range and variance were used to measure the dispersion between the soil parameters. The skewness and kurtosis were used to measure the asymmetry of the soil parameters and describes the extent of the degree of flatness. The descriptive statistics were conducted using Unscrambler 10.4 software.

3. Results and discussion

3.1. Soil properties

Summary statistics for the soil samples of Triffa plain, including minimum, maximum, mean, Standard Deviation (SD), variance, median, range, skewness and kurtosis are shown below (Table 1). The SOM content of the reference dataset is ranged from 1.12% to 3.30% with a mean of 2.27% and an SD of 0.5. The skewness of 0.90 and a kurtosis of 0.56 indicate that the SOM content of dataset has a normal distribution. According to the SOM results of samples, the soils of Triffa plain are characterized by low to medium SOM contents (Carr, 2018; Lazaar et al., 2019). The spatial variability of SOM content is probably due to the nature of topsoils (isohumic, rendzina, brown calcareous, fersialitic, less-developed, and hydromorphic soils), soil textures, soil degradation and the percentage of CaCO3 content. Concerning the $CaCO_3$ content, the samples represented a wide range of CaCO3 ranged from 0 to 38.69% with a mean value of 8.72 %. According to the AFNOR NF P 94-048 (2003) norm, the soils in the study area are generally characterized by slightly to moderately calcareous soil classes. Our results confirm those obtained by Lazaar et al. (2019) and Ruellan (1971). The assessment of soil salinity is based on electrical conductivity (EC) data and their spatial distribution. The EC value of soil samples is varied between 0.11 and 0.9 ms/cm, according to Horneck, Sullivan, Owen, and Hart (2011), the soils of Triffa plain are characterized by low salinity. Soil pH ranged from 6.94 to 7.84 with a mean value of 7.39. Following the soil pH range edited by Horneck et al. (2011), the soils in the study area are considered moderately alkaline (95% soil samples) and others are neutral (5% soil samples). The results of our work confirmed those obtained by Bendra et al. (2012) and Lazaar et al. (2019). The available phosphorus of soil samples varied from 0.45 to 357.68 ppm with a mean of 74.73 ppm. According to Horneck et al. (2011), the Triffa plain is characterized by soils with a wide range of available phosphorus content varied between low (3%), medium (10%), high (80) and excessive.

Also statistics for the SOM content in all soil samples used in the calibration and validation models of the two measurement setups is varied between 1.12 and 3.30% for the calibration samples and 1.5 to 3.27 for the validation samples (Table 1).

3.2. Comparison between soil spectra and data pre-treatment

The results of the two measurement setups (CP) and (PG) of soil spectra showed that all soil samples have similar reflectance spectra in the range between 400 and 2450 nm, where the reflectance was generally lower in the VIS range (400–780 nm) and higher in the NIR range (781–2450 nm). These spectra present two small absorption peaks appear at 430 nm and 530 nm in the visible range, due to the presence of iron oxides and blue colour absorption bands (Sherman & Waite, 1985; Tekin, Tumsavas, & Mouazen, 2012). In the NIR range, three distinct absorption peaks are

Table 1
Descriptive statistics of soil chemical analysis (n = 115 soil samples) and SOM distribution in analysed samples used in the calibration and validation models.

	Descriptive statistics soil chemical analysis (N = 115 soil samples)					SOM (%) distribution in analysed samples used in the calibration and validation models for the PG and CP configurations	
	P_5O_2 (ppm)	pH	EC (ms/cm)	$CaCO_3$ (%)	SOM (%)	Calibration (N = 85 soil samples)	Validation (N = 30 soil samples)
Mean	74.738	7.399	0.388	8.721	2.270	2.20	2.20
Max	357.682	7.840	0.964	38.690	3.300	3.30	3.27
Min	0.458	6.940	0.116	0	1.127	1.12	1.50
Standard Deviation	78.349	0.199	0.197	8.427	0.547	0.547	0.507
Variance	6138.563	0.039	0.038	71.025	0.300	0.300	0.327
Median	48.113	7.400	0.364	5.952	2.262	2.262	2.195
Range	357.225	0.900	0.848	38.690	2.172	2.172	1.907
Skewness	1.996	-0.018	0.667	-0.224	0.902	0.028	-0.263
Kurtosis	3.727	-0.782	-0.164	-0.419	0.568	-0.980	-0.872

present around 1415 nm, 1915 nm and 2200 nm (Fig. 3a and Fig. 3b). The absorption at 1415 nm and 1915 nm is strong and caused by absorption atmospheric of moisture (Nocita et al., 2014; Whiting, Li, & Ustin, 2004) and the presence of both hydration and crystallization water (vibrational frequencies of\OH groups in the water) (Bishop, Pieters, & Edwards, 1994). While the peak near 2200 nm is due to the absorption of Al–OH and clay minerals (Viscarra Rossel & Behrens, 2010). In the range between 2000 and 2450 nm, a clear difference in reflectance spectra is marked for the both setups (CP and PG), according to Bishop et al., (1994) that's can be due to the characteristics of soil organic matter and clays minerals.

Comparing the reflectance intensity for the two measurement setups: The spectral curves obtained by the pistol grip configuration of these soils have a greater reflectance intensity than contact probe configuration. The differences in reflectance spectra and their intensity between the two laboratory setups can be due to the standard protocol and conditions for measuring soil spectra, problems related to unstable illumination, personnel may have negative consequences and affect comparability of the results and other environmental conditions (Schaepman & Dangel, 2000; Viscarra Rossel et al., 2006).

Moreover, the differences in reflectance spectra and their intensity between the soil samples of each setup separately can attributed to the variations in the SOM content and other soil properties (Table 1). Fig. 4 describes the results of the first derivate with Savitzky-Golay method obtained in the pre-treatment step.

3.3. Results of cross-validation and independent validation and SOM mapping

The results of the model performance statistics are summarized in Table 2 and Fig. 5, which plot the laboratory measured and predicted SOM concentrations using PLSR analysis for the calibration and validation data sets.

The pistol grip (PG) measurement setup gives the best calibration quality (R^2 = 0.90) for the SOM content, compared to the contact probe measurement setup (R^2 = 0.84). This performance is stronger than that found by (Rosero-vlasova et al., 2016) for SOM with R^2 = 0.77 for the pistol grip setup and R^2 = 0.74 for the contact probe setup. The RMSE obtained with the PLSR method is 0.17 and 0.24 for the SOM, respectively, with the pistol grip and the contact probe setups, which shows the better quality of the model. On the other hand, the contact probe setup is the widely accessories used in VIS-NIR soil spectroscopy by many authors (Kawamura et al., 2017; Tümsavaş, 2017; Xu et al., 2016) in order to predict soil proprieties compared to the pistol grip with illuminator lamp configuration. However, in our study, the better results were obtained by the pistol grip setup rather than the contact probe setup, which accords with (Rosero-vlasova et al., 2016).

The accuracy of results of the independent validation models are given in Table 2 and Fig. 5. The PLSR models of the pistol grip and contact probe setups have a coefficient of determination of 0.93 and 0.85 respectively and a root means square error (RMSE) of 0.13 for the pistol grip (PG) setup and 0.19 for the contact probe (CP). These

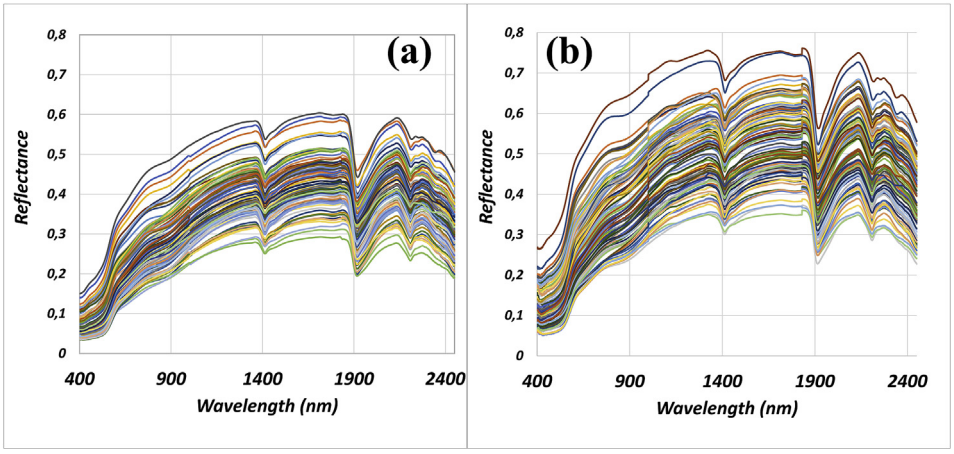

Fig. 3. Spectra of soil samples as measured by the contact probe (a) and pistol grip (b) configurations.

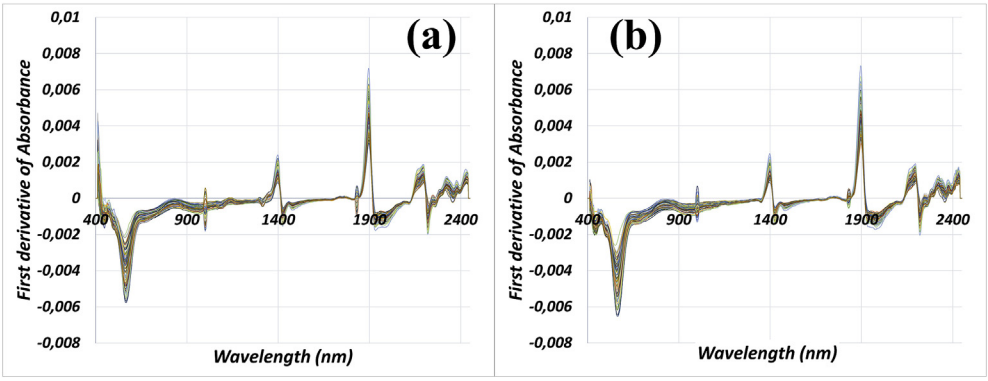

Fig. 4. Pre-treatment of the NIR spectra ((a): contact probe configuration; (b): pistol grip configuration).

Table 2
The performance of the calibrated models according to the two strategies (CP and PG) used to measure the spectral data.

	Calibration		Validation	
	R^2_{Cal} (%)	RMSE $_{Cal}$	R^2_{Val} (%)	RMSE $_{Val}$
(PG) Configuration	0.90	0.17	0.93	0.13
(CP) configuration	0.80	0.24	0.85	0.19

values of R^2 and RMSE of the independent validation are above and better comparatively than those achieved by the corresponding calibrations. This result demonstrates the positive and the higher quality of calibration and validation models in order to estimate the SOM in all soil samples. The models based on the pistol grip setup showed a high predictive accuracy of SOM with variance of 90% compared to the contact probe configuration. From our study, we suggest the researchers for using the pistol gripe setups in the laboratory for the SOM prediction in order to confirm our results.

The main objective of mapping of SOM with the IDW interpolation is to compare the map of laboratory reference measurements with the map of the two setups of laboratory Vis-NIR spectroscopy prediction in the study area. The results of this IDW interpolation of the measured and predicted SOM with the contact probe and pistol grip setups are shown in Fig. 7. Comparing the map of the spatial distribution of SOM results by the two measurement setups of spectroscopy (pistol grip setup (Fig. 6b) and contact probe setup (Fig. 6c) referred to the map of measured SOM with the traditional laboratory method (Walkley–Black) (Fig. 6a), show the high spatial similarity of the predicted models of SOM with the two setups of Vis-NIR spectroscopy, compared with the reference measurement in the laboratory. In addition, the grip pistol setup method with a coefficient of determination $R^2 = 0.93$ and root mean square error (RMSE) of 0.13, provide a higher prediction of SOM relative to the contact probe setup with R2 = 0.85 and RMSE of 0.19. A minor difference in the spatial distribution of SOM is observed in the north-eastern part of the study area for the contact probe setup. Therefore, the grip pistol setup of the Vis-NIR spectroscopy system used in this study can be considered as a promising and accurate tool to provide intensive information of SOM and offers a map with much-improved detail, compared to the traditional laboratory analyses, which are complicated, expensive and time consuming.

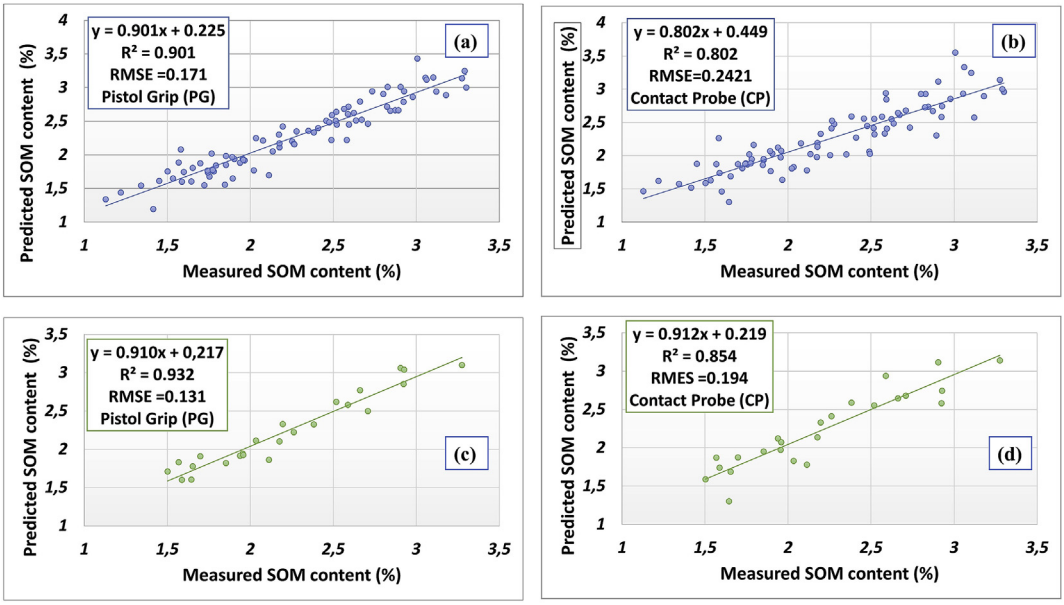

Fig. 5. Scatter plots of measured against predicted values of SOM content based on the PLSR method of the calibration and validation set for both setups the pistol grip (PG) and contact probe (CP): The graphics (a) and (b) corresponding to the results of the PLSR method for the calibration data of the (PG) and (CP) setups respectively. Also, the graphics (c) and (d) corresponding to the PLSR results of validation data for the (PG) and (CP) setups respectively.

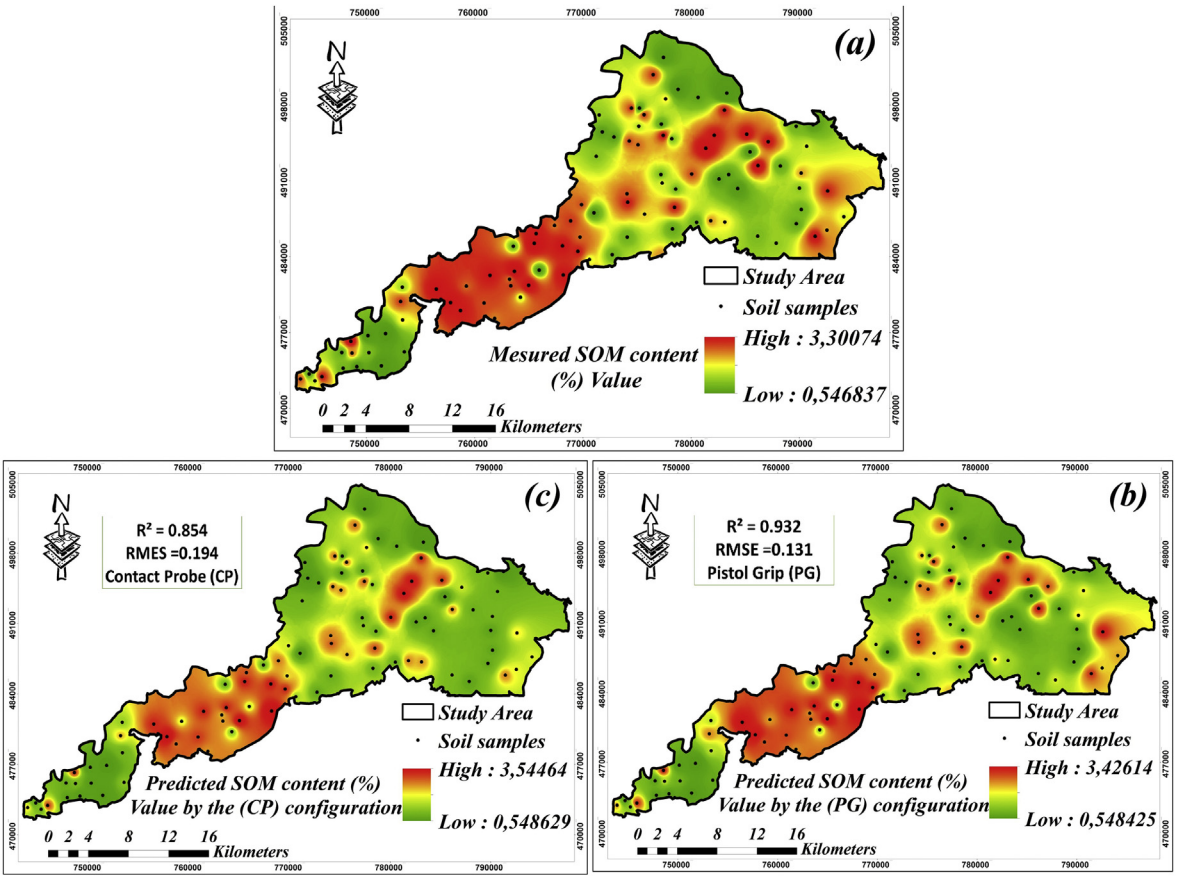

Fig. 6. Maps comparison of Spatial distribution of SOM content between the measured SOM in laboratory (a) and predicted SOM by data of Vis-NIR spectroscopy for the two measurement setups pistol grip (b) and Contact probe (c).

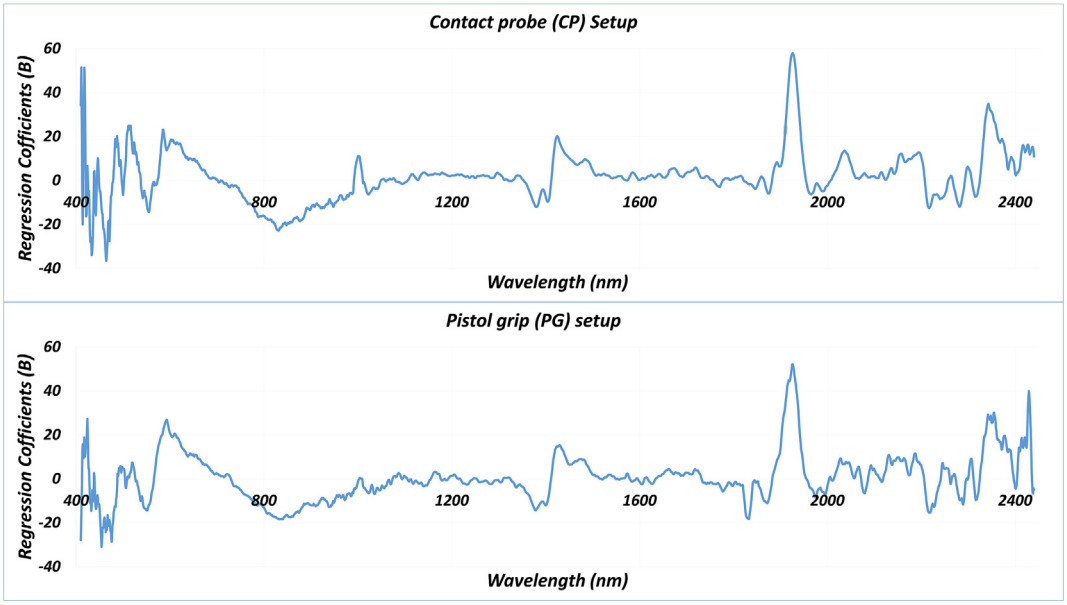

Fig. 7. B coefficient curves obtained from PLSR analyses of the two measurement setups (Contact probe (CP) and Pistol grip (PG)).

3.4. Correlation coefficients of wavelengths

The contribution of each band of the VIS-NIR spectral range of the SOM content prediction models is distinct from the b coefficient of PLSR. The regression coefficients (or b coefficient) summarizes the association between all predictors and a given response and provide information about the importance of the X-variables. Tekin et al., 2012 indicated that the plot of coefficient regression illustrates the importance of wavelengths associated with properties, in this case of our study SOM content. Fig. 7 shows the regression coefficient of the two laboratory setups CP and PG from the cross-validation PLSR analysis for SOM.

Comparing the regression coefficient curves of the contact probe configuration with the pistol grip configuration in the range between 400 and 2450 nm reveals substantial similarities, particularly for significant absorption wavelengths 1430, 1929 and 2220 nm. The wavelengths appear at 1430 nm and 1920 nm were related to water absorption (Hong et al., 2018; Mouazen et al., 2007; Nocita et al., 2014; Viscarra; Viscarra Rossel & Behrens, 2010), and the wavelength appears at 2200 nm due to the lattice OH in clay minerals (Nocita et al., 2014; Viscarra; Viscarra Rossel & Behrens, 2010).

For the pistol grip (PG) setup, the most important peaks used to predict SOM are situated in the visible range for the wavelengths 424, 500, 521 and 597 nm and in the NIR range for the wavelength 840, 1379, 1432, 1484, 1830, 1920, 2200, 2357 and 2430 nm. Concerning the contact probe (CP) setup the important peaks appear in the visible range for the wavelengths 433, 470, 483, 517, 553, 587 and 615 nm, and in the NIR range for 830, 1004, 1380, 1431,1929, 2041, 2200 and 2345 nm.

In the visible range, the significant wavelengths at 424 nm for (PG) and 433, 470 and 483 nm for (CP) setups can be attributed to blue colour absorption (Tekin et al., 2012). The absorbance peak near 500 nm, 521 and 597 nm for the (PG) and near 517, 553 and 587 nm for the (CP) setups be could due to the chromophore FeOOH found in goethite, free iron oxides and small amounts of hematite (Fe2O3) (Ben-Dor et al., 2008; Viscarra; Mortimore, Marshall, Almond, Hollins, & Matthews, 2004; Viscarra Rossel & Behrens, 2010). In the NIR region, the band found at 840 nm and 830 nm for (PG) and (CP) setups respectively can be associated to the chromophorous constituents iron oxides mainly hematite and goethite (Sherman & Waite, 1985) and to the SOM content (Ben-Dor, Irons, & Epema, 1999). The highest correlation b coefficients were observed in the range between 1000 and 2450 nm for both setups (CP and PG). The featured absorption bands around 1379, 1432, 1484, 1830 and 1920 nm for the (PG) and 1380, 1431, 1830, 2041 and 2200 nm for the (CP) setups were considered in detail for their relationships with clay, soil water content, and SOM content (Hong et al., 2018; Mouazen et al., 2007; Nocita et al., 2014; Viscarra Rossel & Behrens, 2010; Thomasson, Sui, Cox, & Al–Rajehy, 2001). The wavelengths appear at 2357 nm and 2430 nm for the (PG) and 2345 nm for the (CP) configurations can be attributed to Al–OH bend plus O–H stretch combinations, that are diagnostic absorption features in clay mineral identification (Clark, King, Klejwa, Swayze, & Vergo, 1990). From the discussion above it can be concluded that the near infrared (NIR) spectrum were more accurate than those in the visible (VIS) spectral range for predicting SOM using both setups (contact probe(CP) and grip pistol (PG)), which confirms the results obtained by Miloš and Bensa (2017). The significant wavelengths contributing to the prediction of SOM for the pistolet grip (PG) setup were at 424, 597, 1432, 1484, 1830, 1920, 2200, 2357 and 2430 nm, while were at 433, 587, 1380, 1431, 1929, 2200 and 2345 nm for the contact probe setup (CP).

4. Conclusions

The present study demonstrated the ability of the combined application of soil Vis-NIR spectroscopy and the PLSR method to analyse and predict the SOM of the soils of the Triffa Plain of north-east Morocco using two laboratory setups, the contact probe (CP) and pistol grip (PG) and the IDW interpolation method for mapping. The mains conclusions are:

1) Vis-NIR spectroscopy is a useful tool for predicting the SOM in the irrigated perimeter of Triffa Plain.
2) The pistol grip setup gives the highest calibration quality for SOM content compared to the contact probe measurement setup.
3) The PLSR is widely and most used method for spectral calibration and prediction, because it gives more stronger correlated results of SOM with the laboratory Vis-NIR spectroscopy measurements.
4) The pistol grip setup measurement of the Vis-NIR spectroscopy system used in this study can be considered as a promising and accurate tool to provide intensive information on SOM. Is offers a map with much-improved detail, compared to the contact probe setup and to the traditional laboratory analyses which are complicated, expensive and time consuming.

Declaration of competing interest

The authors declare that they have no known competing financial interests or personal relationships that could have appeared to influence the work reported in this paper.

Acknowledgments

The authors acknowledge the facilities and financial supports provided by the Mohammed First University and the National Institute of Agronomic Research (INRA) of Oujda. I want to thank all researchers of the Applied Geosciences Laboratory and all researchers of INRA for his help in collecting the soil samples and their analysis in the laboratory.

References

AFNOR NF P 94-048. (2003). *Sols : Recognition and testing - determination of carbonate content - calcimeter method*.

Aïchi, H., Fouad, Y., Walter, C., Viscarra Rossel, R. A., Lili Chabaane, Z., & Sanaa, M. (2009). Regional predictions of soil organic carbon content from spectral reflectance measurements. *Biosystems Engineering, 104*(3), 442–446. https://doi.org/10.1016/j.biosystemseng.2009.08.002.

Aubert, G. (1965). Soil classification: Tables of classes, subclasses, groups and subgroups of soils used by the ORSTOM pedology section. *ORSTOM notebook: Pedology Series, III*, 269–288.

Bao, N., Wu, L., Ye, B., Yang, K., & Zhou, W. (2017). Assessing soil organic matter of reclaimed soil from a large surface coal mine using a field spectroradiometer in laboratory. *Geoderma, 288*, 47–55. https://doi.org/10.1016/j.geoderma.2016.10.033.

Barnes, R. J., Dhanoa, M. S., & Lister, S. J. (1989). Standard normal variate transformation and de-trending of near-infrared diffuse reflectance spectra. *Applied Spectroscopy, 43*(5), 772–777. https://doi.org/10.1366/0003702894202201.

Bellon-Maurel, V., Fernandez-Ahumada, E., Palagos, B., Roger, J. M., & McBratney, A. (2010). Critical review of chemometric indicators commonly used for assessing the quality of the prediction of soil attributes by NIR spectroscopy. *Trends in Analytical Chemistry, 29*(9), 1073–1081. https://doi.org/10.1016/j.trac.2010.05.006.

Ben-Dor, E., & Banin, A. (1990). Near-infrared reflectance analysis of carbonate concentration in soils. *Applied Spectroscopy, 44*(6), 1064–1069. https://doi.org/10.1366/0003702904086821.

Ben-Dor, E., Irons, J., & Epema, G. (1999). Soil reflectance. In A. N. Rencz (Ed.), *Remote sensing for the earth sciences: Manual of remote sensing* (pp. 111–188). New York: USA.

Ben-Dor, E., Ong, C., & Lau, I. C. (2014). Reflectance measurement of soils in the laboratory : Standards and protocols. *Geoderma, 245–246*, 112–124. https://doi.org/10.1016/j.geoderma.2015.01.002.

Ben-Dor, E., Taylor, R. G., Hill, J., Demattê, J. A. M., Whiting, M. L., Chabrillat, S., et al. (2008). Imaging spectrometry for soil applica tions. *Advances in Agronomy, 97*, 321–392. https://doi.org/10.1016/S0065-2113(07)00008-9, 07.

Bendra, B., Fetouani, S., Laffray, X., Vanclooster, M., Sbaa, M., & Aleya, L. (2012). *Effects of irrigation on soil physico-chemistry : A case study of the Triffa plain (Morocco)*. Irrigation and drainage. https://doi.org/10.1002/ird.688.

Bishop, J. L., Pieters, C. M., & Edwards, J. O. (1994). Infrared spectroscopic analyses on the nature of water in montmorillonite. *Clays and Clay Minerals, 42*, 702–716.

Bogrekci, I., & Lee, W. S. (2004). Spectral signatures of common phosphates in soils and their effect on absorbance spectra of soil samples with different phosphorus concentrations. *Annual International Meeting*, 1–12. https://doi.org/10.13031/2013.16739.

Carr, M. (2018). Hidden hunger and intelligent guesswork. In *Advances in tea agronomy* (pp. 253–276). https://doi.org/10.1017/9781316155714.014.

Chang, C. W., Laird, D. A., Mausbach, M. J., & Hurburgh, C. R. (2001). Near-Infrared reflectance spectroscopy–principal components regression analyses of soil properties. *Soil Science Society of America Journal, 65*(2), 480. https://doi.org/10.2136/sssaj2001.652480x.

Chen, H., Pan, T., Chen, J., & Lu, Q. (2011). Waveband selection for NIR spectroscopy analysis of soil organic matter based on SG smoothing and MWPLS methods. *Chemometrics and Intelligent Laboratory Systems, 107*(8), 139–146. https://doi.org/10.1016/j.chemolab.2011.02.008.

Clark, R. N., King, T. V. V., Klejwa, M., Swayze, G., & Vergo, N. (1990). High spectral resolution reflectance spectroscopy of minerals. *Journal of Geophysical Research, 95*(B8), 12653–12680. https://doi.org/10.1029/JB095iB08p12653.

Coûteaux, M. M., Berg, B., & Rovira, P. (2003). Near infrared reflectance spectroscopy for determination of organic matter fractions including microbial biomass in coniferous forest soils. *Soil Biology and Biochemistry, 35*(12), 1587–1600. https://doi.org/10.1016/j.soilbio.2003.08.003.

Curcio, D., Ciraolo, G., D'Asaro, F., & Minacapilli, M. (2013). Prediction of soil texture distributions using VNIR-SWIR reflectance spectroscopy. *Procedia Environmental Sciences, 19*, 494–503. https://doi.org/10.1016/j.proenv.2013.06.056.

Demattê, J. A. M., Ramirez-Lopez, L., Marques, K. P. P., & Rodella, A. A. (2017). Chemometric soil analysis on the determination of specific bands for the detection of magnesium and potassium by spectroscopy. *Geoderma, 288*(February), 8–22. https://doi.org/10.1016/j.geoderma.2016.11.013.

Fekkoul, A. (2012). Groundwater contamination by nitrates, salinity and pesticides: Case of the unconfined aquifer of Triffa plain (eastern Morocco). *Revue Marocaine Des Sciences Agronomiques et Vétérinaires, 2*, 12–36. https://doi.org/10.4409/Am-034-11-0034.

Fystro, G. (2002). The prediction of C and N content and their potential mineralisation in heterogeneous soil samples using Vis–NIR spectroscopy and comparative methods. *Plant and Soil, 246*(2), 139–149. https://doi.org/10.1023/A.

Gholizadeh, A., Borůvka, L., Saberioon, M., & Vasat, R. (2013). Mid-Infrared spectroscopy applications for soil assessment with emphasis on soil organic matter content and quality. *Applied Spectroscopy OA, 67*(12), 1349–1362. https://doi.org/10.1366/13-07288.

Gholizadeh, A., Carmon, N., Klement, A., Ben-Dor, E., & Borůvka, L. (2017). Agricultural soil spectral response and properties assessment: Effects of measurement protocol and data mining technique. *Remote Sensing, 9*(10), 1–14. https://doi.org/10.3390/rs9101078.

Gomez, C., Lagacherie, P., & Coulouma, G. (2008a). Continuum removal versus PLSR method for clay and calcium carbonate content estimation from laboratory and airborne hyperspectral measurements. *Geoderma, 148*(2), 141–148. https://doi.org/10.1016/j.geoderma.2008.09.016.

Gomez, C., Oltra-Carrió, R., Bacha, S., Lagacherie, P., & Briottet, X. (2015). Evaluating the sensitivity of clay content prediction to atmospheric effects and degradation of image spatial resolution using Hyperspectral VNIR/SWIR imagery. *Remote Sensing of Environment, 164*, 1–15. https://doi.org/10.1016/j.rse.2015.02.019.

Gomez, C., Viscarra Rossel, R. A., & McBratney, A. B. (2008b). Soil organic carbon prediction by hyperspectral remote sensing and field vis-NIR spectroscopy: An Australian case study. *Geoderma, 146*(3–4), 403–411. https://doi.org/10.1016/j.geoderma.2008.06.011.

He, Y., Song, H., Pereira, A. G., & Gómez, A. H. (2005). Measurement and analysis of soil nitrogen and organic matter content using near-infrared spectroscopy techniques. *Journal of Zhejiang University - Science, 6B*(11), 1081–1086. https://doi.org/10.1631/jzus.2005.B1081.

Hong, Y., Chen, S., Zhang, Y., Chen, Y., Yu, L., Liu, Yanfang, et al. (2018). Rapid identification of soil organic matter level via visible and near-infrared spectroscopy: Effects of two-dimensional correlation coefficient and extreme learning machine. *The Science of the Total Environment, 644*, 1232–1243. https://doi.org/10.1016/j.scitotenv.2018.06.319.

Horneck, D. a, Sullivan, D. M., Owen, J. S., & Hart, J. M. (2011). *Soil test interpretation guide*. Oregon State University, Extension Service. https://doi.org/10.1017/CBO9781107415324.004. July.

Jakab, G., Rieder, Á., Vancsik, A. V., & Szalai, Z. (2018). Soil organic matter characterisation by photometric indices or photon correlation spectroscopy: Are they comparable? *Hungarian Geographical Bulletin, 67*(2). https://doi.org/10.15201/hungeobull.67.2.1.

Ji, W., Adamchuk, V. I., Biswas, A., Dhawale, N. M., Sudarsan, B., Zhang, Y., et al. (2016). Assessment of soil properties in situ using a prototype portable MIR spectrometer in two agricultural fields. *Biosystems Engineering, 152*, 14–27. https://doi.org/10.1016/j.biosystemseng.2016.06.005. December 2017.

Jiang, Q., Chen, Y., Guo, L., Fei, T., & Qi, K. (2016). Estimating soil organic carbon of cropland soil at different levels of soil moisture using VIS-NIR spectroscopy. *Remote Sensing, 8*(9). https://doi.org/10.3390/rs8090755.

Kawamura, K., Tsujimoto, Y., Rabenarivo, M., Asai, H., Andriamananjara, A., & Rakotoson, T. (2017). Vis-NIR spectroscopy and PLS regression with waveband selection for estimating the total C and N of paddy soils in Madagascar. *Remote Sensing, 9*(10). https://doi.org/10.3390/rs9101081.

Lagacherie, P., Baret, F., Feret, J. B., Madeira Netto, J., & Robbez-Masson, J. M. (2008). Estimation of soil clay and calcium carbonate using laboratory, field and airborne hyperspectral measurements. *Remote Sensing of Environment, 112*(3), 825–835. https://doi.org/10.1016/j.rse.2007.06.014.

Lavelle, P., Barot, S., Blouin, M., Decaëns, T., Jimenez, J. J., & Jouquet, P. (2007). Earthworms as key actors in self-organized soil systems. *Theoretical Ecology Series, 4*(C). https://doi.org/10.1016/S1875-306X(07)80007-4.

Lazaar, A. (2016). *The contribution of hyperspectral remote sensing in the soil characterization of the Triffa Plain (Eastern Morocco)* (Master's thesis). Oujda, Morocco: Mohammed First University.

Lazaar, A., Mahyou, H., Gholizadeh, A., Elhammouti, K., Bilal, M., Andich, K., et al. (2019). Potential of VIS-NIR spectroscopy to characterize and discriminate topsoils of different soil types in the Triffa plain (Morocco). *Soil Science Annual, 70*(1). https://doi.org/10.2478/ssa-2019-0007.

Leone, A., Viscarra-Rossel, R. A., Amenta, P., & Buondonno, A. (2012). Prediction of soil properties with PLSR and vis-NIR spectroscopy: Application to Mediterranean soils from southern Italy. *Current Analytical Chemistry, 8*, 283–299. https://doi.org/10.2174/157341112800392571.

Memon, M. S., Guo, J., Tagar, A. A., Perveen, N., Ji, C., Memon, S. A., et al. (2018). The effects of tillage and straw incorporation on soil organic carbon status, rice crop productivity, and sustainability in the rice-wheat cropping system of eastern China. *Sustainability, 10*(March), 1–14. https://doi.org/10.3390/su10040961.

Miloš, B., & Bensa, A. (2017). Prediction of soil organic carbon using VIS-NIR spectroscopy : Application to Red Mediterranean soils from Croatia. *Eurasian Journal of Soil Science, 6*(4), 365–373. https://doi.org/10.18393/ejss.319208.

Mortimore, J. L., Marshall, L. J. R., Almond, M. J., Hollins, P., & Matthews, W. (2004). Analysis of red and yellow ochre samples from Clearwell Caves and Catalhoyuk by vibrational spectroscopy and other techniques. *Spectrochimica Acta Part A: Molecular and Biomolecular Spectroscopy, 60*(5), 1179–1188. https://doi.org/10.1016/j.saa.2003.08.002.

Mouazen, A. M., Kuang, B., De Baerdemaeker, J., & Ramon, H. (2010). Comparison among principal component, partial least squares and back propagation neural network analyses for accuracy of measurement of selected soil properties with visible and near infrared spectroscopy. *Geoderma, 158*(1–2), 23–31. https://doi.org/10.1016/j.geoderma.2010.03.001.

Mouazen, A. M., Maleki, M. R., De Baerdemaeker, J., & Ramon, H. (2007). On-line measurement of some selected soil properties using a VIS-NIR sensor. *Soil and Tillage Research, 93*(1), 13–27. https://doi.org/10.1016/j.still.2006.03.009.

Mouazen, A. M., Saeys, W., Xing, J., De Baerdemaeker, J., & Ramon, H. (2005). Near infrared spectroscopy for agricultural materials: An instrument comparison. *Journal of Near Infrared Spectroscopy, 13*(2), 87–97. https://doi.org/10.1255/jnirs.461.

Nawar, S., & Mouazen, A. M. (2017). Predictive performance of mobile vis-near infrared spectroscopy for key soil properties at different geographical scales by using spiking and data mining techniques. *Catena, 151*(December), 118–129. https://doi.org/10.1016/j.catena.2016.12.014.

Nocita, M., Stevens, A., Toth, G., Panagos, P., van Wesemael, B., & Montanarella, L. (2014). Prediction of soil organic carbon content by diffuse reflectance spectroscopy using a local partial least square regression approach. *Soil Biology and Biochemistry, 68*, 337–347. https://doi.org/10.1016/j.soilbio.2013.10.022.

Powlson, D. S., Brookes, P. C., Whitmore, A. P., Goulding, K. W. T., & Hopkins, D. W. (2011). Soil organic matters. *European Journal of Soil Science, 62*(1), 1–4. https://doi.org/10.1111/j.1365-2389.2010.01338.x.

Rayment, G. E., & Higginson, F. R. (1992). *Australian laboratory handbook of soil and water chemical methods*. Australia: Inkata Press.

Rosero-vlasova, O. A., Péerez-Cabello, F., Lloveria, R. M., & Vlassova, L. (2016). Assessment of laboratory VIS-NIR-SWIR setups with different spectroscopy accessories for characterisation of soils from wildfire burns. *Biosystems Engineering*, 1–17. https://doi.org/10.1016/j.biosystemseng.2016.06.011.

Ruellan, A. (1971). *Soils with a differentiated calcareous profile of the plains of lower Moulouya (Eastern Morocco)*. Paris: FR: OROSTOM.

Sacko, B. D., Sanogo, S., Konare, H., Ba, A., & Diakite, T. (2018). Capability of visible-near infrared spectroscopy in estimating soils carbon, potassium and phosphorus. *Optics and Photonics Journal*, 123–134. https://doi.org/10.4236/opj.2018.85012, 08(05).

Savitzky, A., & Golay, M. J. E. (1964). Smoothing and differentiation of data by simplified least squares procedures. *Analytical Chemistry, 36*(8), 1627–1639. https://doi.org/10.1021/ac60214a047.

Schaepman, M. E., & Dangel, S. (2000). Solid laboratory calibration of a nonimaging spectroradiometer. *Applied Optics, 39*(21), 3754–3764. https://doi.org/10.1364/AO.39.003754.

Sherman, D. M., & Waite, T. D. (1985). Electronic spectra of Fe3 + oxides and oxide hydroxides in the near IR to near UV. *American Mineralogist, 70*, 1262–1269.

Six, J., Conant, R. T., Paul, E. A., & Paustian, K. (2002). Stabilization mechanisms of soil organic matter: Implications for C- saturation of soils. *Plant and Soil, 241*,

155–176. https://doi.org/10.1023/A.
St Luce, M., Ziadi, N., Zebarth, B. J., Grant, C. A., Tremblay, G. F., & Gregorich, E. G. (2014). Rapid determination of soil organic matter quality indicators using visible near infrared reflectance spectroscopy. *Geoderma, 232–234*, 449–458. https://doi.org/10.1016/j.geoderma.2014.05.023.
Stevens, A., Udelhoven, T., Denis, A., Tychon, B., Lioy, R., Hoffmann, L., et al. (2010). Measuring soil organic carbon in croplands at regional scale using airborne imaging spectroscopy. *Geoderma, 158*(1–2), 32–45. https://doi.org/10.1016/j.geoderma.2009.11.032.
Stevens, A., Van Wesemael, B., Vandenschrick, G., Touré, S., & Tychon, B. (2006). Detection of carbon stock change in agricultural soils using spectroscopic techniques. *Soil Science Society of America Journal, 70*, 844–850. https://doi.org/10.2136/sssaj2005.0025.
Sun, W., Li, X., & Niu, B. (2018). Prediction of soil organic carbon in a coal mining area by Vis-NIR spectroscopy. *PLoS One, 13*(4), 1–10. https://doi.org/10.1371/journal.pone.0196198.
Tekin, Y., Tumsavas, Z., & Mouazen, A. M. (2012). Effect of moisture content on prediction of organic carbon and pH using visible and near-infrared spectroscopy. *Soil Science Society of America Journal, 76*(1), 188. https://doi.org/10.2136/sssaj2011.0021.
Thomasson, J. A., Sui, R., Cox, M. S., & Al–Rajehy, A. (2001). Soil reflectance sensing for determining soil properties in precision agriculture. *Transactions of the ASAE, 44*(6), 1445–1453. https://doi.org/10.13031/2013.7002.
Tümsavaş, Z. (2017). Application of visible and near infrared reflectance spectroscopy to predict total nitrogen in soil. *Journal of Environmental Biology, 38*, 1101–1106. https://doi.org/10.22438/jeb/38/5(SI)/GM-29, 5(SI).
Tümsavaş, Z., Tekin, Y., Ulusoy, Y., & Mouazen, A. M. (2018). Prediction and mapping of soil clay and sand contents using visible and near-infrared spectroscopy. *Biosystems Engineering*, 1–12. https://doi.org/10.1016/j.biosystemseng.2018.06.008.
Van Waes, C., Mestdagh, I., Lootens, P., & Carlier, L. (2005). Possibilities of near infrared reflectance spectroscopy for the prediction of organic carbon concentrations in grassland soils. *Journal of Agricultural Science, 143*(6), 487–492. https://doi.org/10.1017/S0021859605005630.
Vašát, R., Kodešová, R., Borůvka, L., Klement, A., Jakšík, O., & Gholizadeh, A. (2014). Consideration of peak parameters derived from continuum-removed spectra to predict extractable nutrients in soils with visible and near-infrared diffuse reflectance spectroscopy (VNIR-DRS). *Geoderma, 232–234*, 208–218. https://doi.org/10.1016/j.geoderma.2014.05.012.
Virgawati, S., Mawardi, M., Sutiarso, L., Shibusawa, S., Segah, H., & Kodaira, M. (2018). Mapping the variability of soil texture based on VIS-NIR proximal sensing. *Journal of Applied Geospatial Information, 2*(1), 108–116. https://doi.org/10.30871/jagi.v2i1.798.
Viscarra Rossel, R. A., & Behrens, T. (2010). Using data mining to model and interpret soil diffuse reflectance spectra. *Geoderma, 158*(1–2), 46–54. https://doi.org/10.1016/j.geoderma.2009.12.025.
Viscarra Rossel, R. A., Walvoort, D. J. J., McBratney, A. B., Janik, L. J., & Skjemstad, J. O. (2006). Visible, near infrared, mid infrared or combined diffuse reflectance spectroscopy for simultaneous assessment of various soil properties. *Geoderma, 131*(1–2), 59–75. https://doi.org/10.1016/j.geoderma.2005.03.007.
Walkley, A., & Black, I. A. (1934). An examination of the degtjareff method for determining soil organic matter, and a proposed modification of the chromic acid titration method. *Soil Science, 37*(1), 29–38. https://doi.org/10.1097/00010694-193401000-00003.
Whiting, M. L., Li, L., & Ustin, S. L. (2004). Predicting water content using Gaussian model on soil spectra. *Remote Sensing of Environment, 89*(4), 535–552. https://doi.org/10.1016/j.rse.2003.11.009.
Xie, H. T., Yang, X. M., Drury, C. F., Yang, J. Y., & Zhang, X. D. (2011). Predicting soil organic carbon and total nitrogen using mid- and near-infrared spectra for Brookston clay loam soil in Southwestern Ontario, Canada. *Canadian Journal of Soil Science, 91*(1), 53–63. https://doi.org/10.4141/cjss10029.
Xu, G. C., Li, Z. B., Li, P., Lu, K. X., & Wang, Y. (2013). Spatial variability of soil organic carbon in a typical watershed in the source area of the middle Dan River, China. *Soil Reasearch, 51*(1), 41–49. https://doi.org/10.1071/SR12327.
Xu, S., Shi, X., Wang, M., & Zhao, Y. (2016). Effects of subsetting by parent materials on prediction of soil organic matter content in a hilly area using vis-NIR spectroscopy. *PLoS One, 11*(3), 1–17. https://doi.org/10.1371/journal.pone.0151536.